

**THERMAL ENERGY STORAGE WITH MOLTEN SALT THERMOCLINE**

**Giampaolo Caputo, Irena Balog, Giuseppe Canneto and Domenico Mazzei**  
ENEA – Energy Technologies Department, Via Anguillarese, 301 – 00123 Rome, Italy

**ABSTRACT**

Thermal storage with molten salt is considered to be an important subsystem for solar thermal power plants due to the fluctuation of sunshine over time. A molten salt thermal storage tank, in which the fluid is stratified in temperature with hot in the upper and cold in the lower level due to the density difference of the fluids. Generally porous media are used to fill the tank in order to reduce the inventory of the molten salt and manage the mixing between the hot and cold molten salt, so as to form a stable layer of thermocline. However, in the flow of molten salt, either the hot fluid displaces the cold one or vice versa, phenomena of viscous fingering and/or channeling are likely to occur, which may disturb the stability of the thermocline, resulting in an over widened temperature transitional zone. In this study no porous media is used. The cold and the hot fluid zone are in direct contact. In this work is studied the analysis of the flow when cold molten salt displaces hot molten. Special attention is given to the thermocline region. Numerical simulation is presented where are find to be useful for the process analysis, for the scale-up of the thermal storage system and to evaluate the system reliability for industrial plants.

**Keywords:** Solar Energy, Thermal Storage, Molten Salt, Stratification

**1. INTRODUCTION**

Thermal energy storage (TES) has been proved an important sub-system for the solar energy generation systems (SEGS) where its performance is considerably increased. This additional step distinguishes the solar thermal power plants from the conventional fossil fuel thermal power plants. A well designed, operated and managed molten salt TES system for SEGS achieves several goals:

- To release energy for electricity generation after sunset for several hours to meet the power consumption peak without the fossil fuel backup, and make the SEGS more independent of the weather fluctuations over time, increasing the efficient annual usage of sunlight.
- To improve the system performance and economic index, such as reduce the levelized electricity cost.

Two types of TES system, in which molten salt was used as the heat transfer fluid (HTF) and also served as the energy storage medium (ESM), have been investigated at ENEA for large scale SEGS application. One of them is the so called two-tank molten salt thermal storage [1-6]. This system was also successfully used for parabolic trough solar plants. Though the two-tank TES system was found to substantially benefit the performance of the SEGS plant and made it

operate much more economically. In order to reduce costs, the single-tank molten salt TES, was chosen to be investigated. A single tank TES used thermocline to separate the hot and cold fluids. It was estimated that the single tank TES system can save 25-30% of investment cost compared to a two-tank storage system [7-8].

A critical aspect that determines the performance of a single-tank TES is the thermocline thickness and its stability. Energy stored in the tank with molten salt may not be fully retrieved in the discharging phase. Mixing of the hot and cold molten salt fluids broadens the thickness of the thermocline and reduces the useful amount of the hot fluid, with which the discharging molten salt must be above a certain temperature to generate superheated steam. Discharge efficiency,  $\eta$ , characterized in the single-tank performance is [9]:

$$\eta = \text{output energy} / \text{total energy stored in the tank}$$

Thermal energy delivered at temperatures greater than a certain value is qualified as useful energy. Different authors found that the discharge efficiency varies depending on the height of the tank and the molten salt flow.

On the other hand, the thermocline thickness in the mixing zone of the hot and cold molten salt is a measure of the charge/discharge efficiency in the single-tank TES system. Mixing or de-stratification of the two HTFs always results in entropy generation, in other words, the internal exergy loss of the TES system. Therefore, exergy loss can be used as a measure of the ability of the TES. The stratification efficiency,  $\varepsilon$ , can be written as [10]:

$$\varepsilon = (\text{Exergy loss of fully mixing} - \text{actual Exergy loss}) / \text{Exergy loss of fully mixing}$$

$\varepsilon = 0$  represents a fully mixing state and  $\varepsilon = 1$  represents an ideal stratification of the two HTFs with different temperatures. There are several factors promoting or degrading stratification [11-12]. The primary driving force for stratification is the density difference or actually the relative density difference. The density of molten salt (Hitec XL) is  $2118 \text{ kg/m}^3$  at  $190 \text{ }^\circ\text{C}$  and  $1943 \text{ kg/m}^3$  at  $450 \text{ }^\circ\text{C}$ , this leads to an absolute density difference of  $175 \text{ kg/m}^3$  or a relative difference of 9,17%. The turbulence and associated mixing in the tank is the primary cause for the degradation of the stratification. A thermocline tank requires thus a well-designed diffuser at the inlet that dissipates the kinetic energy. However, with increasing density differences the ratio between buoyancy and inertia forces becomes more beneficial and the cold fluid enters in the hot storage during a discharging process drop down to bottom, resulting in mixing reduction. The convective mixing currents which occur at the walls are caused by the heat loss and the higher conductivity occurring at the walls which have a much higher impact than the heat loss itself. The fluid cools down at the wall and the higher density leads to a downward flow until the fluid reaches either the fluid with the same density or the bottom of the tank. This causes a compensating flow in the center of the tank to replace the displaced fluid. The mixing of hot and cold fluid layers, the associated entropy generation and exergy loss has much higher impact on the performance than the pure heat loss. Due to the higher temperature difference to the ambient

and the resulting heat loss, the temperature difference between bulk fluid and boundary layer, that is the driving force for the buoyancy current, is much higher for molten salt systems. However, the size of commercial-scale molten salt tanks is reducing the impact of this effect since the shell-area-to-volume-ratio is decreasing with increasing diameters. Those results in the ratio reduction of the wall boundary layer compared to the total tank volume much smaller. In this work a constructive modification inside the tank was studied by computational fluid dynamics (CFD) simulations where first comparison between experimental results and CFD simulation are presented [13].

## **2. MATERIAL AND METHODS**

The prototype tank, represented in Figure 1, contains one spiral heat exchangers. The top exchanger allows the discharging phase where heating up of a cold oil sent to the user.



**Figure 1.**Experimental setup

In the scheme of Figure 2 it is possible to observe the lift channel connecting (adiabatically) the top to the bottom of the tank.

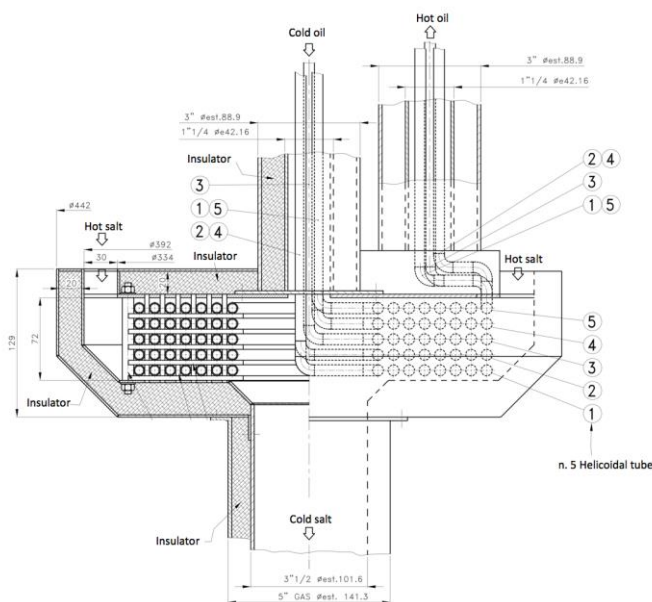


**Figure 2.**Heat exchanger and channel

The heat exchangers, visible in Figure 3, are composed by a series of coil connected in parallel with the oil flowing on the tube sides and the molten salts (MS) on the shell side.



**Figure 3.**Picture of the spiral heat exchangers

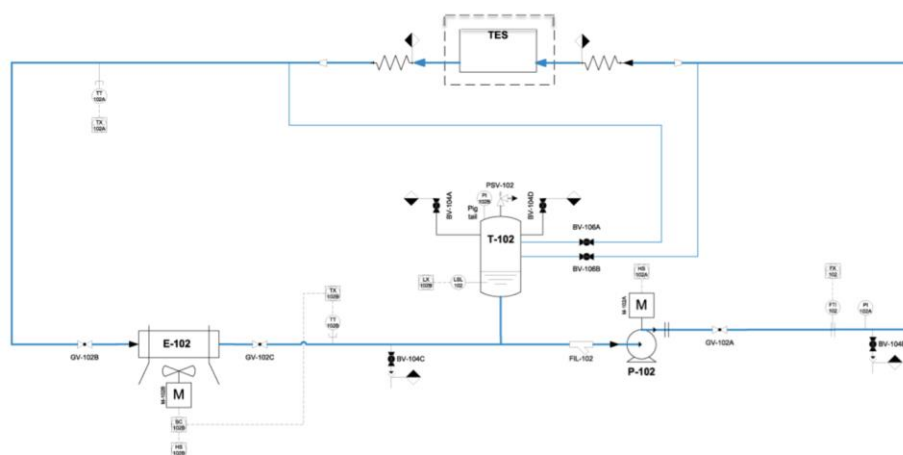
The geometry is summarized in the table 1:

**Table 1: Geometry of heat exchanger and tank**

coil number	5
L coil	4,72 m
De coil	0,009525 m
S coil	0,00124 m
A	0,706 m <sup>2</sup>
H tank	1,9 m
D tank	0,784 m
V tank	0,9 m <sup>3</sup>

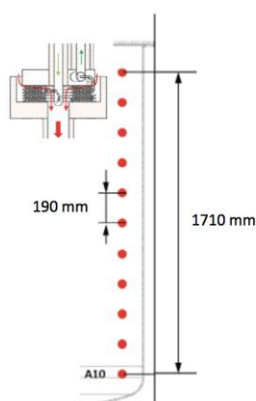
A complete test is characterized by an initial heating phase of the salt and a subsequent discharging phase. It is possible to have the two phases at the same time in order to keep a constant temperature distribution of the salt inside the tank.

In the discharging phase, the cold oil enters from the top of the tank and flows inside the tube where the discharging heat exchanger cools the hot molten salts conveyed from the top of the tank into the shell of the heat exchanger. The cooled molten salts start a natural circulation inside the duct arriving at the bottom of the tank, while the heated oil exits from the heat exchanger at the top of the tank. The experimental apparatus devoted to verify the correct operation of the storage system in its discharging phases, represented in Figure 4.



**Figure 4.**P&I of the discharging circuit

In the experimental apparatus are included a flow meter and two thermocouples to measure the oil flow rate and the temperature (to and from the TS tank). These two measurers allow us to calculate the thermal power transferred to the oil. A temperature sensor controls the velocity of the air fin cooler to cool down the oil returning to the tank. Ten thermocouples are integrated inside the tank presented in Figure 5 giving the ability to analyze the axial temperature distribution and the thermocline trend during the discharge phases.

**Figure 5.**Thermocouples in the tank

The circuit has been filled with the oil and the tank with the salt and some preliminary tests have been carried out to verify the correct working of the pilot plant (starts from the loading and melting phase and the variation of oil mass flow rates to verify the actual presence of the thermocline). When the system become stable, after about an hour, sacks (25 kg) of calcium nitrate, potassium nitrate and sodium nitrate are loaded into the pilot plant to get the composition of the ternary salt of this study. The solid salt was melted and heated to 290 ° C, Figure 6, by an immersed electric resistance which was then removed. In the following tests, the temperatures measured by end thermocouples (the first at the bottom and the last at the top) are not considered because those thermocouples are affected by fluctuations influenced with boundary fluid dynamics of the molten salts.

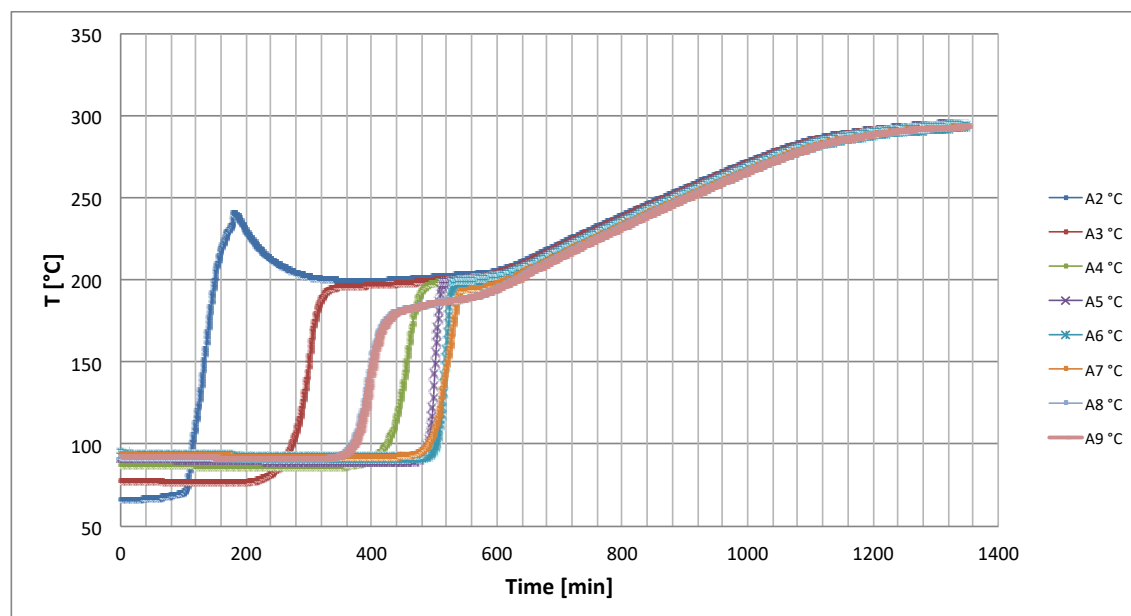


**Figure 6.** Temperature in the tank

The discharging tests have the duration of 15-25 minute and an oil mass flow rate set in the range 300-1000 kg/h. The cold oil flows inside the spiral heat exchanger at the temperature of 180 °C and then it sets on a temperature between 245 °C and 250 °C. The hot molten salts inside the tank has an initial average temperature of 290 °C and reaches the average temperature of 280 °C by heating the oil flowing through the exchanger. The oil used is Dowtherm Q.

### 3. RESULT AND DISCUSSION

#### 3.1 Experimental results

In discharge phase the thermal energy stored in the molten salt is transferred through the heat exchanger to the cold oil. The cold oil (420 kg/h) enters from above, through a pipe that flows in the central part and feeds the 5 coil of the exchanger connected in parallel. The hot oil is cooled to 180 °C in the air heater. In the Figure 7 is showed the oil temperature.

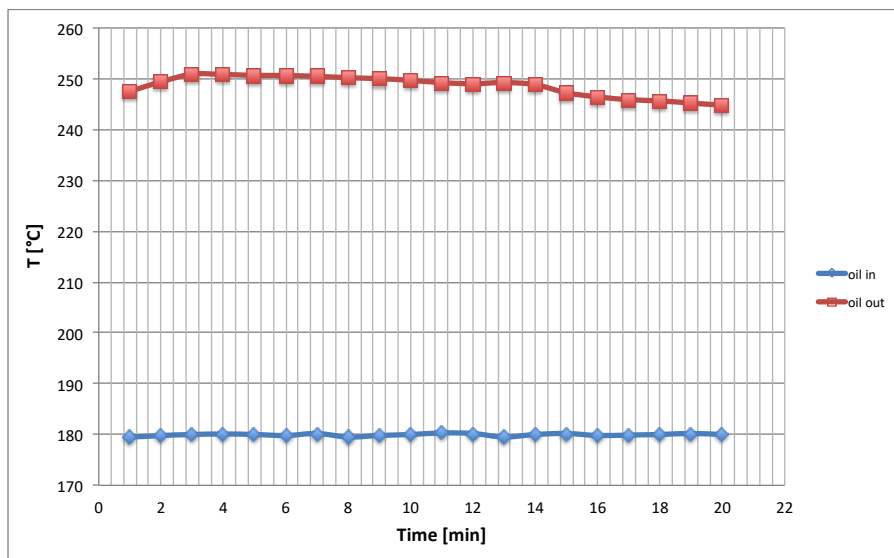


Figure 7.Oil temperature

The hot salt enters the upper part and passes through the coils, crossed against the oil, yields heat, cooling and triggering a circulation that carries the salt through the discharge channel in the lower part of the tank, Figure 8.

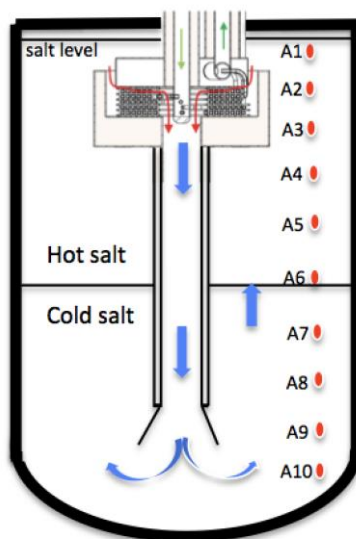


Figure 8.Discharge phase

Figure 9 shows the temperatures along the tank as a function of time.

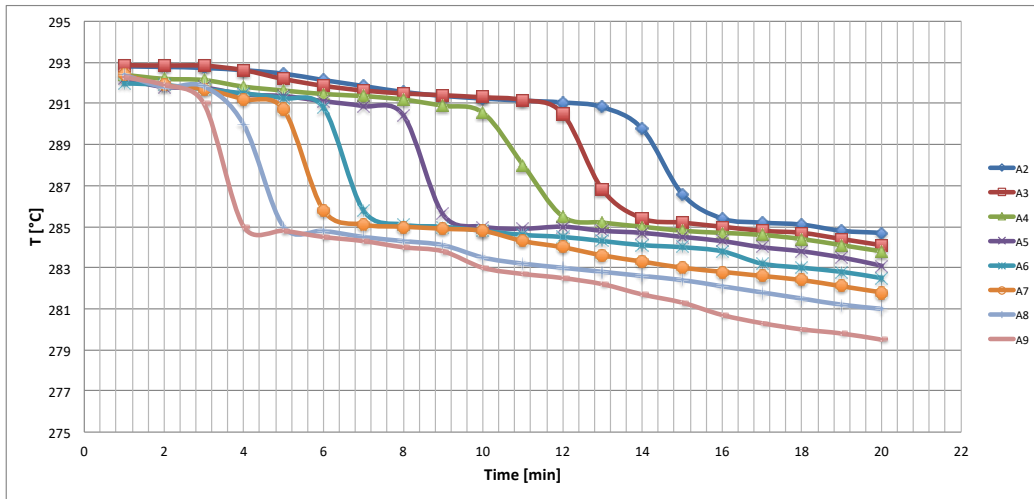
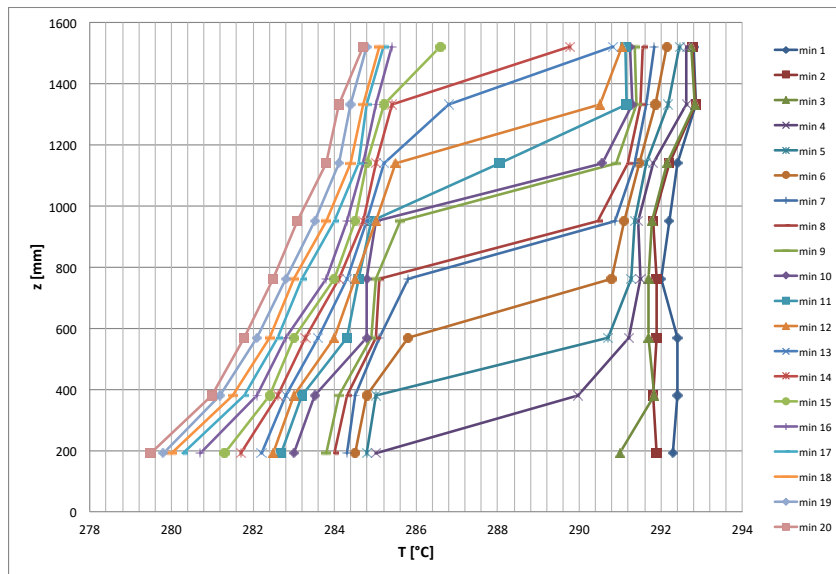


Figure 9. Temperature vs time in the tank

Figure 10 shows the temperatures along the height of the tank.



**Figure 10.**Temperature along the tank

Hereby, having available temperature and flow rate of the oil in the circuit of the heat exchangers, it has been possible to validate a model of the Shell & Tube type heat exchangers with the helicoidal heat exchanger installed inside the TES. The natural circulation inside the TES allowed us to measure an exchanged thermal power and a stationary oil flow rate. The temperature profile in the tank is detected nearby 9 thermocouples. Temperatures are detected every minute.

Applying the energy balances for oil and salt it was possible check the molten salt mass flow involved, Figure 11.

$$Q = F \cdot U \cdot A \cdot \Delta T_{ml} \quad (1)$$

where:

Q = heat exchanged [W]

F = corrective factor

U = global heat exchange coefficient [W/m<sup>2</sup>\*K]

A = heat exchange surface [m<sup>2</sup>]

$\Delta T_{ml}$  = logarithmic mean temperature difference [K]

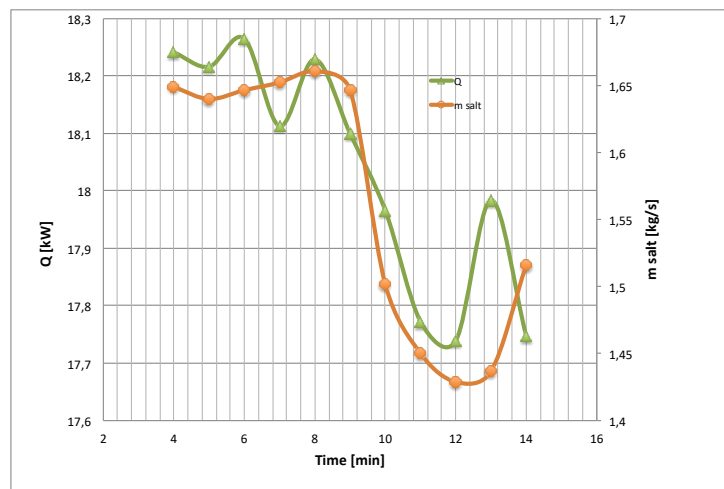


**Figure 11.**Power and molten salt flow

The global heat exchange coefficient has the contribution of the thermal resistance of the films of the individual fluids (oil and salt) and the conductive part that affects the material (interposed between the two fluids) of which the exchanger is formed. Out of these definitions, with the usage of the experimental results, it is possible to calculate the heat transfer coefficient of the salt.

Validation is performed and the exchange coefficient  $U_{cis}$  calculated compared with the measurable value  $U_d$  (estimated from the energy balance) as in the classic Kern design algorithm.

In (1) the corrective factor  $F$  often appears which, based on the actual heat exchange profile reduces the logarithmic mean temperature difference (LMTD); it is estimated on the basis of the cross-flow model with the value of 0,97. In the calculation of the LMTD, the measurements in time of the temperature of the bottom salts (thermocouple A9) and of the head detected on the thermocouple A2 were used.

The shell side exchange coefficients,  $h_o$ , and tube side  $h_{io}$ , are estimated from the reports for the Nusselt number calculation,  $Nu$ . The thermal exchange equations in forced convection depend on the physical properties of the fluids and on the volumetric flow of the salts inside the coils (heat exchanged with the oil). In the Table 2 is summarized the results (medium value) of the discharge phase.

**Table 2: Results discharge**

test	Q [kW]	$m_s$ [kg/s]	$h_o$ [W/m <sup>2</sup> K]	$h_{io}$ [W/m <sup>2</sup> K]	$U_d$ [W/m <sup>2</sup> K]	$U_c$ [W/m <sup>2</sup> K]
Discharge	18	1,5	498	1698	392	401

### 3.2 CFD simulation

**A simplified geometry is considered in order to study the heat transfer and the fluid flow problem as 2D, axisymmetric. Only a half 2D geometric modelling is considered in the study, where the problem is symetric. The modelling includes the tank, the discharging helicoidal heat exchanger and the 3 1/2 inches pipeneeded to transfer the cold molten salts from the top, at the exit of the heat exchanger, to the bottom zone of the tank. The main objective of the numerical simulation is to investigate the time-evolution of bulk MS stratification during discharge.**

The Cad module included in the software Ansys14.5® is used to build the geometry, while for the grid the automatic meshing module has been used. The computational domain is discretized into finite volumes. The total number of cells is approximately 115000 with an average orthogonal

quality equal to 0,986. The tank has a 0,784 m diameter and is about 2 m high. Figure 12 shows the considered geometry and one of the used computational grid.

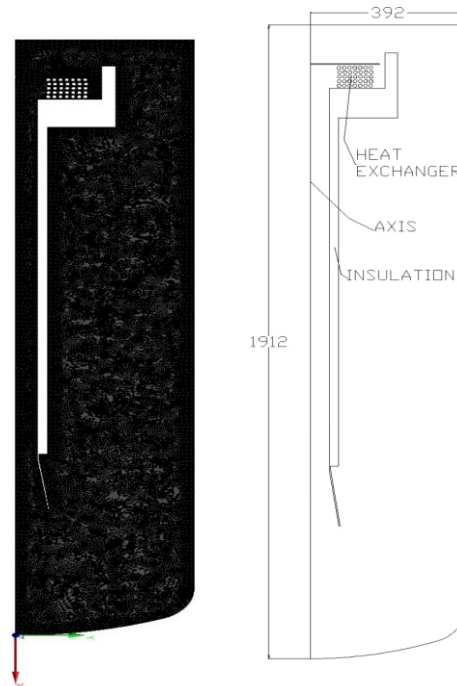


**Figure 12.**The geometry and the grid

The mixture of salts is Hitec XL has the following properties:

$$C_p(T) = 1544,18 - 0,326 * T \text{ [J/Kg*K]},$$

$$\rho(T) = 2240,05 - 0,8226 * T \text{ [Kg/m}^3\text{]}$$

$$K(T) = 0,005 * T + 0,4 \text{ [W/m*K]}$$

$$\mu(T) = \exp [-10,71 + 2895,76 / (T + 273,15 - 60,36)] \text{ [Pa*s]}$$

At the beginning of the discharging process, it is assumed that the tank is filled with MS at a temperature of 292 °C with a zero velocity throughout the domain. No-Slip condition is considered for all the walls.

A zero heat flux boundary condition is assigned to all walls except the discharge exchanger walls where a user-defined function (UDF, i.e. a “C” routine) is implemented with the aim of considering the change of the heat flux with wall temperature. A UDF is used to calculate the molecular viscosity of the MS. Different simulations were carried out to inspect the dependence

of the results from different grid densities and time intervals. The computations are performed using the CFD module FLUENT [14].

A second-order implicit scheme is used for time discretization, second-order upwind for momentum and energy discretization with weighted body forced for pressure discretization. Pressure–velocity coupling is implemented through the PISO algorithm. Iterations at each time step are terminated when the dimensionless residuals for all flow equations drop below  $10^{-4}$  and energy residual drops below  $10^{-7}$ . Considering the properties of the fluid and the geometry of the tank the Rayleigh number is lower than  $10^9$ , so the flow in the tank is considered laminar. The analysis is carried out considering a total heat transfer rate of 18 kW in the discharge exchanger at the beginning of the simulation. The total simulated time is 47,4 minute. Throughout the simulation, it is noted that, already after about 20 minute the temperature in the upper part of the tank, at the inlet of the discharge exchanger, begins to decrease. This condition is well described in Figure 13 where the temperature contour after 22 minute from the beginning of the transient is shown.

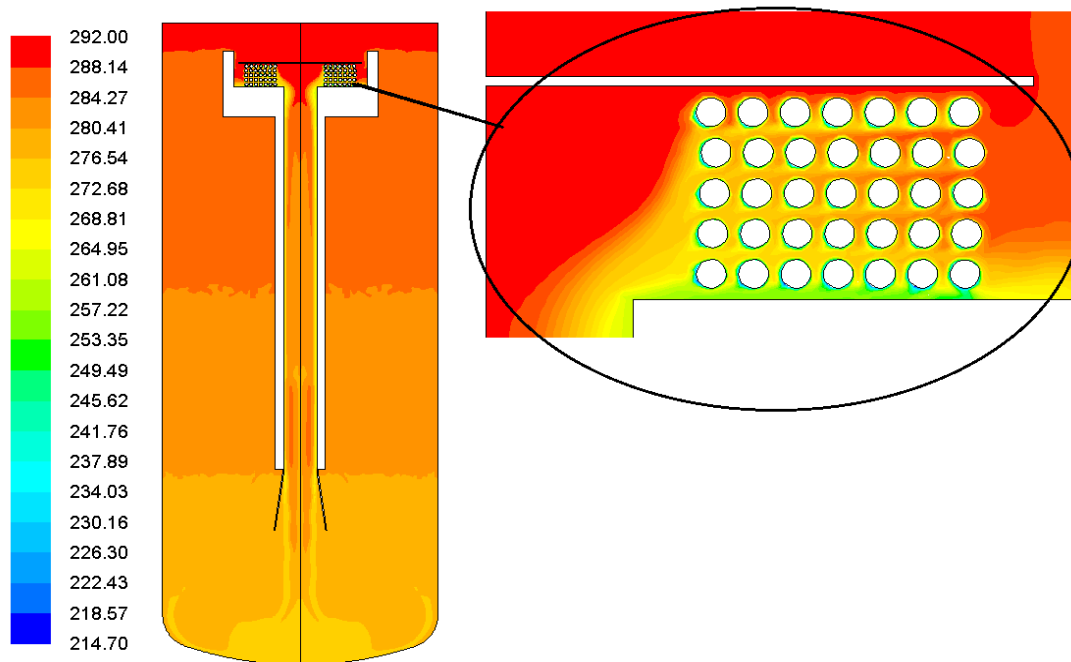


**Figure 13.**The temperatures contour after 22 minutes

It is possible to notice in detail that the maximum temperature difference between the entrance and the exit of the heat exchanger is about 30 °C.

In addition, graphs with the temperature propagation along the tank (positioned section line as in the Figure 8) Figure 14 and Figure 15, to make a comparison with the similar experimental curves in Figure 9 and Figure 10.

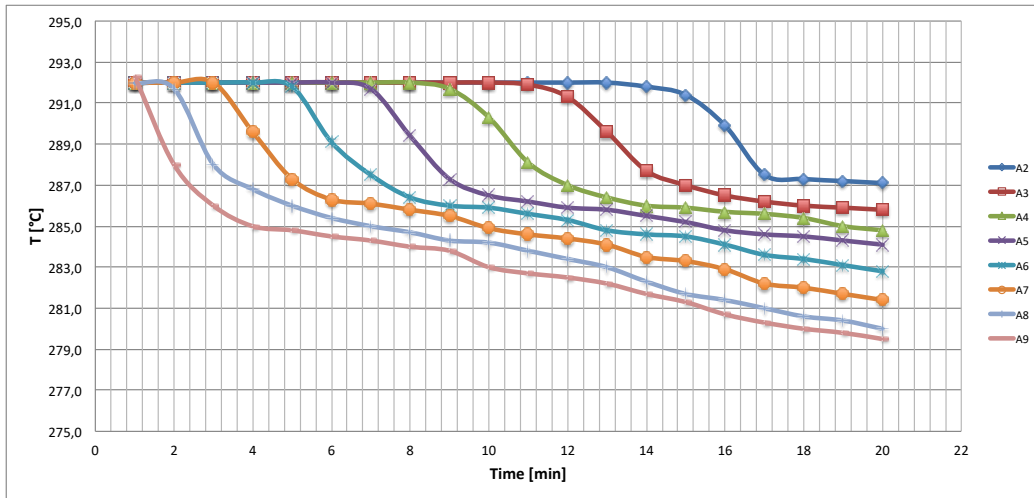


Figure 14. Temperatures vs time in the tank

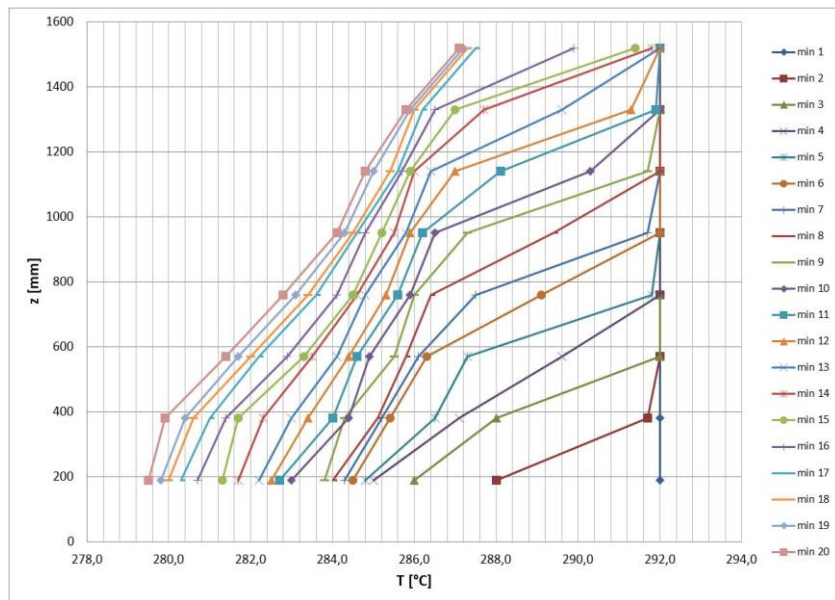


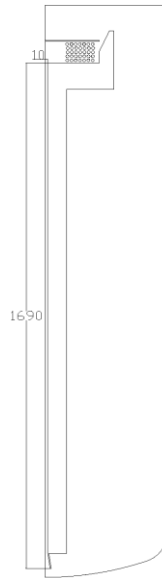
Figure 15. Temperature along the tank

The simulation, as the experimental tests, shows a lowering of the salt temperature smaller than the expected value.

Further on, in order to obtain lower temperatures at the exit of the exchanger and therefore a longer discharge time it was decided to perform a second simulation with a modified geometry of the tank.

The diameter and the length of the central tube have been modified; the diameter reduced to 0,02 m, the length increased to 1,69 m. Moreover, in order to improve the flow and therefore the heat exchange of the coils in the upper part of the exchanger, the entrance wall has been tilted.

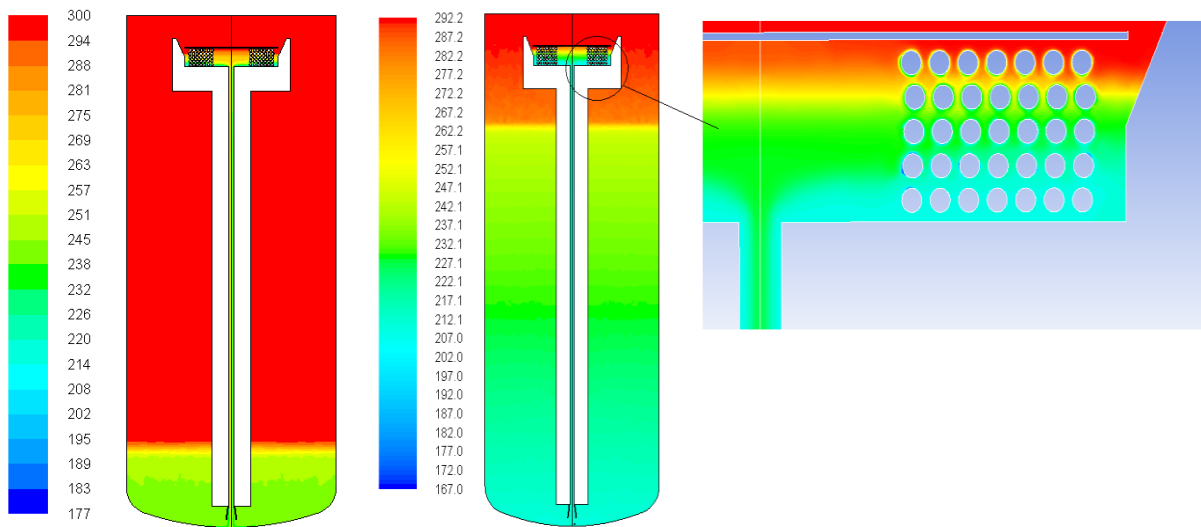
The second simulation is carried out for a total time of 3 hours and 10 minute. In this case the simulation starts with an initial salt temperature equal to 300 ° C but with the same exchange power (18 kW) considered in the first simulation. In Figure 1 is presented the new geometry used for the simulation.



**Figure 16.**Geometry used in the second simulation

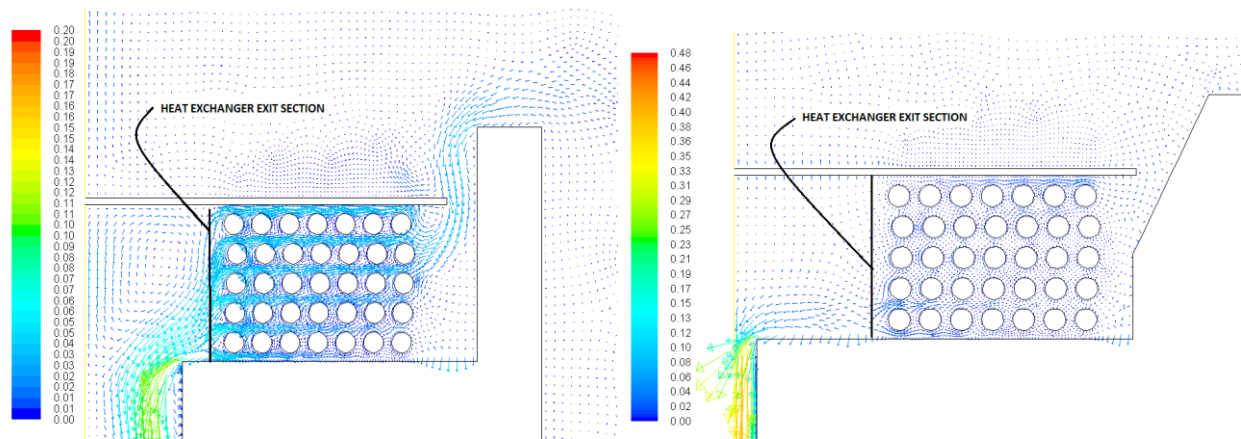
As in the first simulation it was obtained the temperature contour at 22 min to make a comparison with the real geometry.

Figure 17 shows the temperature maps after 22 min and at the end of the simulation (3 h and 10 min).



**Figure 17.**Temperature contours at 22 min (left) and at 3 h 10 min with a detail of the exchanger zone(right)

In this case the max temperature difference between the inlet and the exit of the heat exchanger is about 80 ° C.The different behavior of the salt flow can be observed also in Figure 18 where the map of the velocities in the exchanger zone, for both simulations, are shown.



**Figure 18.** Velocity vectors map in the heat exchanger zone

Consider the output section of the heat exchanger, the average value (surface integral) of the radial velocity has been calculated where a value of  $V_y = -0,0153$  m/s has been found in the first simulation and a value of  $V_y = -0,002675$  m/s in the modified second simulation geometry.

This remarkable difference justifies the greater temperature difference in the exchanger which is obtained in the case of the modified geometry.

The length of the thermocline region is a measure of the thermal stratification inside the tank; the quality of the energy stored in the tank decreases as this length increases (poor stratification) [15].

Figure 19 compares the different heights of the heat-exchange zone at the same minute (22th) for the first simulation (left) and for the second simulation (right).

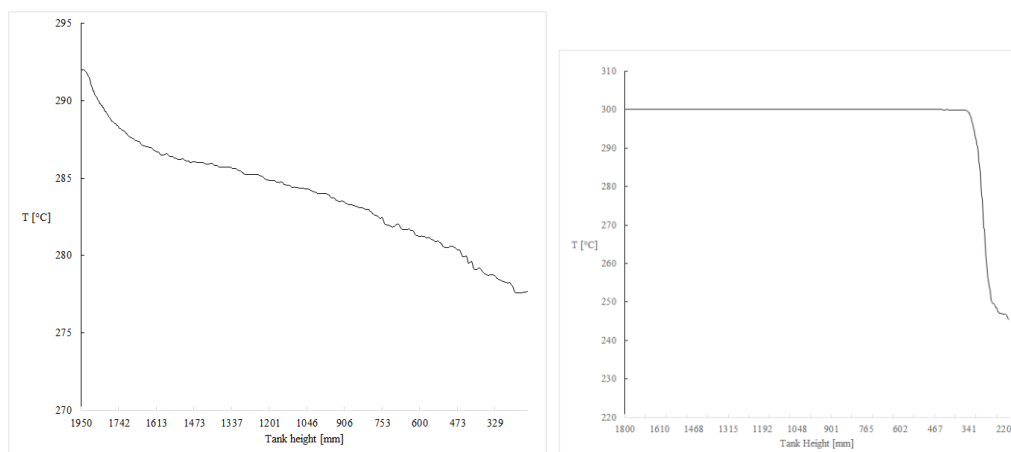


**Figure 19.** Different heights of the thermocline at the same minute (22) for the first simulation (left) and for the second simulation (right).

As it can be observed in Figure 19, in the second simulation the height of thermocline region is only about 0,2 m.

#### 4. CONCLUSION

The first stratification results have been obtained with the oil loop and single-tank storage prototype patented and built in ENEA. The first tests have been performed with lower temperature differences. The total temperature change in the tank takes place in only 15 minute where the absolute temperature difference is 16 °C. Even though, the stratification process is very good, it can be observed that the thermocline is increasing in the discharge process which could be related to elevate molten salt flow in the heat exchanger. The study of the correct

geometry and therefore the flow rate of the molten salt inside the heat exchanger are fundamental.

Within the CFD study this compromise was found. With the modified geometry the temperature difference between the entrance and the exit of the heat exchanger is about 80 °C instead of 30 °C obtained in the original geometry. It was found that the thermocline region is much narrower and ultimately the complete discharge of the tank takes more than 3 hours compared to the 15 minute of the original geometry.

## Acknowledgment

The computing resources and the related technical support used for this work have been provided by CRESCO/ENEAGRID High Performance Computing infrastructure and its staff [16]. CRESCO/ENEAGRID High Performance Computing infrastructure is funded by ENEA, the Italian National Agency for New Technologies, Energy and Sustainable Economic Development and by Italian and European research programmes, see <http://www.cresco.enea.it/english> for information"

## REFERENCES

- [1] ENEA Report Solar Thermal Energy Production 2001 ENEA/TME/PRES
- [2] Herman et al., Two-tank molten salt storage for parabolic trough solar power plant; Energy 2004; 29:883.
- [3] Pacheco et al., Development of a Molten-Salt Thermocline Thermal Storage System for Parabolic Trough Plants (2002) Journal of Solar Energy Engineering.
- [4] Brosseau et al., Testing of thermocline filler materials and molten-salt heat transfer fluids for thermal energy storage systems in parabolic trough power plants. Sol Energy EngTrans ASME 2005;127:109–16.
- [5] Kearney et al. Assessment of a molten salt heat transferfluid in a parabolic trough solar field. J Solar Energy Eng 2003;125:170–6.
- [6] Frank et al., Thermocline stability criterions in single-tanks of molten salt thermal energy storage; Applied Energy 2012; 97:816.
- [7] Flueckinger et al., An integrated thermal and mechanical investigation of molten salt thermocline energy storage; Applied Energy 2011; 88:2098.
- [8] Yang Zhen et al., Molten salt thermal energy storage in thermoclines under different environmental boundary conditions; Applied Energy 2010; 87: 3322.
- [9] Yang Zhen et al., Thermal analysis of solar thermal energy storage in molten salt thermocline, Solar Energy, 2010:84.

- [10] Haller et al., Methods to determine stratification efficiency of thermal energy storage processes – Review and theoretical comparison; *Solar Energy* 2009; 83: 1847.
- [11] Dincer et al., *Thermal energy storage: systems and applications*. John Wiley & Sons, 2002.
- [12] Bernhard et al., Experimental results from a laboratory-scale molten salt thermocline storage, *AIP Conference Proceedings* 1850, 080025 (2017).
- [13] Seubert et al., Numerical investigation and improvement of the standby performance of thermocline storages, *Proceedings of the 20th SolarPACES*, Beijing, 2014.
- [14] ANSYS.Fluent 14.5.0 2011.
- [15] C. Mira-Hernández et al., Numerical simulation of single- and dual-media thermocline tanks for energy storage in concentrating solar power plants, *EnergyProcedia* 2014; 49: 916.
- [16] G. Ponti et al., "The role of medium size facilities in the HPC ecosystem: the case of the new CRESCO4 cluster integrated in the ENEAGRID infrastructure", *Proceedings of the 2014 International Conference on High Performance Computing and Simulation, HPCS 2014*, art. no. 6903807, 1030-1033;